

## Short Communication

# Approximation of Harry Dym Equation *via* Local RBF Method

Hameed Ullah Jan<sup>a\*</sup>, Tahir Khan<sup>a</sup>, Irshad Ali Shah<sup>b</sup> and Muhammad Zubair Khan<sup>a</sup>

<sup>a</sup>Department of Mathematics, University of Science and Technology Bannu, Khyber Pakhtunkhwa-28100, Pakistan

<sup>b</sup>Department of Physical and Numerical Sciences, Qurtuba University of Science and Information Technology, Peshawar-25120, Pakistan

(received September 9, 2023; revised December 26, 2023; accepted January 2, 2024)

**Abstract.** Differential equations, which can be found in many branches of physics and engineering which are produced through mathematical modeling of many physical systems. A crucial dynamical equation that has uses in a number of physical systems is the HD equation. This is one of the significant nonlinear evolution equation that comes up when studying solitons. In this paper, the HD equation is numerically solved using a local radial basis function (LRBF) approach with the goal of creating local spatial approximation at each point in space as a consequence of local methodology. To deal with time variable, Runge-Kutta scheme of order four is applied. For proving suggested method accuracy and efficiency some error norms *viz*  $L_{RMS}$ ,  $L_{\infty}$  and  $L_2$  of test problems are calculated. The solutions obtained by LRBF method are also compared to past studies, and the results of proposed approach are better and more closely match to the exact solution.

**Keywords:** partial differential equations (PDEs), harry dym (HD) equation, meshfree approach, RBF methods, local-RBF method

Engineering, technology and applied sciences phenomena like mechanics and gravity are all described by PDEs with non-linearities. Non-linear PDEs are typically helpful tools that can be used in a range of areas to simulate nonlinear dynamic phenomena including fluid dynamics, solid state physics, mathematical biology and plasma physics. The shallow water propagation is explained by a number of well-known completely integral PDEs, like Boussinesq, Korteweg and De-Vries (KdV) (Korteweg *et al.*, 1895), Whitham-Broer-Kaup (WBK) (Broer, 1975; Kaup, 1975; Whitham, 1967) and Kadomtsev and Petviashvili (KP) (Kupershmidt, 1985; Kadomtsev and Petviashvili, 1970) equations and so forth. The harry dym (HD) equation is a significant dynamical equation that can be integrated and has applications in a number of physical systems. Kruskal and Moser (1975) reported the first to use the HD equation. This is credited to a paper written by Harry between 1973 and 1974. The dym equation illustrates a situation where dispersion and nonlinearity are intertwined. The nonlinear evolution equation known as HD is totally integrable. It is fantastic because, although lacking the Painleve feature, it complies with an unlimited number of conservation laws, bi-hamiltonian

structure and symmetries (Nadjafikhah and Kabi-Nejad, 2013; Gesztesy and Unterkofler, 1992). The KdV equation and the HD equation are closely related and the HD equation also has applicability to hydrodynamics issues (Vasconcelos and Kadanoff, 1991). In addition to these facts, the HD equation is studied in theory of solitons especially and in mathematics (Li and Xu, 2020, Xiao and Fan, 2019; Fuchssteiner *et al.*, 1992). The traditional nonlinear HD equation has been solved by numerous authors using analytical and numerical techniques, see for example (Assabaai, 2021; Assabaai and Mukherij, 2020; Fonseca, 2017; Ghiasi and Saleh, 2017; Rawashdeh, 2014; Mokhtari, 2011; Novikov, 1999; Fuchssteiner *et al.*, 1992).

Meshfree methods are becoming more popular, emerging, interesting and fascinating numerical techniques due to the ability to solve those physical and engineering problems with no meshing or minimum of meshing for which the traditionally used mesh-based methods are not suited like finite volumes, finite differences, finite elements, moving least square, element free galerkin, point interpolation method which also reproducing kernel particle method and boundary element free method. RBFs methods appears to be really consists and most prominent meshless methods among the family of meshless methods, while looking at the

\*Author for correspondence;

E-mail: hameed\_marwat@ustb.edu.pk

interpolation of multidimensional scattered data and have received recently a tremendous and considerable attention in scientific community because of its capacity to achieve spectral accuracy, efficiency and high flexibility in solving complex PDEs, integral equations and fractional equations in comparison to other advanced approaches (Franke and Schaback, 1998a and 1998b; Madych and Nelson, 1992 and 1990; Kansa, 1990a and 1990b; Micchelli, 1984). The most commonly used kernel in meshless techniques is the multi-quadric (MQ) kernel suggested by (Hardy, 1971) using radial basis function to solve PDEs. A localized RBF approach was also separately and concurrently proposed by different authors, which, even today, is a significant and useful finding (Taufiq and Uddin, 2021; Uddin and Taufiq, 2020; Uddin and Taufiq, 2019a and b). The local Kansa approximation approach, the method of approximate particular solution (MAPS) and the method of particular solution (MPS) all uses localized RBFs approach. These methods often produce low conditioned system matrices with decent accuracy. Below Table 1, lists some of RBFs usually used in literature.

**Table 1.** RBFs usually used in literature with their classification

Name and type	$\phi(r)$
Multiquadric (MQ)-RBF	$\sqrt{1+(\zeta r)^2}$
Gaussian (GA)-RBF	$e^{-(\zeta r)^2}$
Thin plate spline (TPS)-RBF	$r^{2\beta \log(r)}$

where:

$\zeta$  an open parameter that has a real value greater than zero. Yet a detailed investigation of the best value for this parameter is currently ongoing and for researchers, it continues to be a challenge (e.g, view the citations (Scheuerer, 2011; Trahan and Wyatt, 2003; Rippa, 1999; Foley, 1994; Tarwater, 1985; Franke, 1982; Hardy, 1971). Localized RBF algorithms are utilized to solve complicated problems on a large scale without the requirement for conditioning. We used the following approach in our calculation to choose an appropriate value of the shape parameter, which is related to the theory of local RBF interpolation.

**Algorithm.** start:  $CNM = 0$ ;  $CNM_{(minimum)} = 10^{12}$ ;  $CNM_{(maximum)} = 10^{16}$ ;

where:

$CNM < CNM_{(minimum)}$  and  $CNM > CNM_{(maximum)}$ ;  $P,Q,R=SVD(S)$ ;  $CNM = \frac{maximum(S)}{minimum(S)}$ ; if,  $CNM < CNM_{(minimum)}$ ,  $\zeta = \zeta - \Delta\zeta$ ;  $CNM > CNM_{(maximum)}$ ,  $\zeta = \zeta + \Delta\zeta$ ; end  $\zeta$  (Best optimal value for shape parameter) =  $\zeta$ ; end

The HD equation in classical order for the aforementioned phenomena appears as:

$$\frac{\partial v(\zeta, \tau)}{\partial \tau} = v^3(\zeta, \tau) \frac{\partial^3 v(\zeta, \tau)}{\partial \zeta^3}, (\zeta, \tau) \in [a,b] \times [0,T] \dots (1)$$

based on given initial condition together with the boundary conditions as follows:

$$v(\zeta, 0) = \rho_0(\zeta) = \rho(\zeta) \dots (2)$$

$$\left\{ \begin{array}{l} v(a, \tau) = q_1(\tau) \\ v(b, \tau) = q_2(\tau) \\ \frac{\partial v(\zeta, \tau)}{\partial \zeta} = r(\tau) \end{array} \right\} \dots (3)$$

where:

$\rho_0, q_1, q_2$  and are the appropriate constants and are the results of equation (1) exact solution, that was stated by (Mokhtari, 2011) as under:

$$v(\zeta, \tau) = [\eta - \frac{3\sqrt{\gamma}}{2} (\zeta + \gamma\tau)^{\frac{2}{3}}] \dots (4)$$

**PDEs via local RBF approach.** We will now discuss a local RBF approximation technique for general time dependent partial differential equations in the spatial domain  $\Omega_s \subset R^s, s \geq 1$  as follows:

$$\left\{ \begin{array}{l} D_\tau v(\zeta, \tau) - Lv(\zeta, \tau) = F(\zeta, \tau), (\zeta, \tau) \in \Omega_s \times (0, T_f) \\ v(\zeta) = v_0, \zeta \in \Omega_s, \tau = 0, \\ Bv(\zeta, \tau) = G(\zeta), \zeta \in \partial\Omega_s, \tau > 0 \end{array} \right\} \dots (5)$$

where:

is the linear differential operator and is the boundary operator, while time domain is represented by  $(0, T_f)$ , where  $T_f$  is the final time.

**Approximation of spatial variable.** Consider  $\{\zeta_1, \zeta_2, \dots, \zeta_N\} \in \Omega \subset R^s, s \geq 1$  as a set of sample data nodes with associated function values  $\{v(\zeta_1), v(\zeta_2), \dots, v(\zeta_N)\} \in R$ , the localized RBF approach at  $\zeta_i \in \Omega$  approximates the function  $v(\zeta_i)$  as follows:

$$v(\zeta_i, \tau) = \sum_{j=1}^N \alpha_j(\tau) \phi(\|\zeta_i - \zeta_j\|_2, \zeta), \zeta_j \in \Omega_i \subset \Omega \subset \mathbb{R}^s, s \geq 1 \dots\dots\dots (6)$$

where:

the nodes  $\zeta$  relate to the region including the neighbouring nodes, the vector of unknown expansion coefficient is represented by  $\alpha_j(\tau) = [\alpha_1(\tau), \dots, \alpha_N]^T$  and  $r = \|\zeta_i - \zeta_j\|_2$  represent the distance between centers  $\zeta_i, \zeta_j$  in Euclidean norm, while  $\phi(r)$  is the RBF function that has been defined for  $r \geq 0$ . As a result, for each local domain  $\Omega_i \subset \Omega$ , following is the N number of  $n \times n$  linear systems:

$$v^i = H^i \alpha^i, i = 1, 2, \dots, N \dots\dots\dots (7)$$

where:

the interpolation matrix  $H^i$  entries are  $k_{kj}^i = \phi(\|\zeta_k - \zeta_j\|_2, \zeta_k - \zeta_j \in \Omega_i)$  and must be solved for determination of unknown coefficients vector  $\alpha_j$ 's. We now have an approximation for the linear differential operator  $\mathcal{L}$  as follows:

$$\mathcal{L}v(\zeta_i, \tau) = \sum_{j=1}^N \alpha_j(\tau) \mathcal{L}\phi(\|\zeta_i - \zeta_j\|_2, \zeta), \zeta_j \in \Omega_i \subset \Omega \subset \mathbb{R}^s, s \geq 1 \dots\dots\dots (8)$$

Equation (8) can be expressed as the dot product of two vectors as under:

$$\mathcal{L}v(\zeta_i, \tau) = K^i \alpha^i \dots\dots\dots (9)$$

where:

the expansion coefficients vector  $\alpha^i$  is of size  $n \times 1$  and  $K^i$  is a vector below with elements that is in size  $1 \times n$

$$K^i = \mathcal{L}\phi(\|\zeta_i - \zeta_j\|_2, \zeta), \zeta_j \in \Omega_i \dots\dots\dots (10)$$

Solving equation (7) for unknown coefficients vector  $\alpha_j$ 's, we have

$$\alpha^i = (H^i)^{-1} v^i \dots\dots\dots (11)$$

Plugging back the values of  $\alpha_j$ 's form equation (11) into equation (9), we obtain

$$\mathcal{L}v(\zeta_i, \tau) = K^i (H^i)^{-1} v^i = M^i v^i \dots\dots\dots (12)$$

where:

$$M^i = K^i (H^i)^{-1} \dots\dots\dots (13)$$

is the weight that corresponds to center  $\zeta_j$ . As a result, we have

$$\mathcal{L}K = Mv \dots\dots\dots (14)$$

where:

the sparse differentiation matrix M has an order of  $N \times N$ . The matrix M has  $N - n$  zeros and non-zero components in each row.

**Approximation of temporal variable.** The following system of ODEs was created after spatial local RBF approximation

$$D_t K = M(v) \dots\dots\dots (15)$$

To discretize equation (15) in time we can use any ODE solver like ode113, ode23 and ode45 from Matlab. The starting vector will be the initial solution  $u_0$ . ode45 is based on an explicit Runge-Kutta (4,5) formula. In general, ode45 is the best function to apply as a first try for most problem. A good ODE solver will automatically select a reasonable time step  $\delta t$  and detect the stiffness of the ODE system. For this ODE computation we will use fourth order Runge-Kutta method and select the time step  $\delta t$  manually.

**Stability of local RBF approach.** Our numerical technique in the current local RBF method of lines (MOL) approach is as under:

$$K_t = Mv \dots\dots\dots (16)$$

A system of time-dependent ODEs is created here from the time-dependent PDE. The concept of using the finite difference method to solve the coupled system of ODEs is known as the "method of lines" (e.g Runge-Kutta, etc.). A rule of thumb is used to look at the stability of lines approach numerically. If the eigenvalues of the time-discretization operator's stability zone, scaled by  $\delta\tau$ , fall inside the boundaries of the linearized spatial discretization operator, the technique of lines is stable (Trefethen, 2000). The eigenvalues for which the method produces a bounded solution make up the complex plane that contains the stability region. Our numerical scheme is described in equation (16) for the current meshless approach of lines. We may examine the stable and unstable eigenvalue spectrum for the above model by calculating the eigenvalues of the matrix M, scaled by  $\delta\tau$ .

**Numerical results.** With the help of error norms  $L_\infty$ ,  $L_2$  and  $L_{RMS}$  outlined below and numerical example, this section aims to demonstrate the remarkable behaviour of our method

$$\left\{ \begin{array}{l} L_\infty = \|v^{\text{exact}} - v^{\text{approx}}\|_\infty = \max |v_i^{\text{exact}} - v_i^{\text{approx}}| \\ L_2 = \|v^{\text{exact}} - v^{\text{approx}}\|_2 = \sqrt{\delta \xi \sum_{i=0}^N |v_i^{\text{exact}} - v_i^{\text{approx}}|^2} \\ L_{RMS} = \sqrt{\frac{\sum_{i=0}^N |v_i^{\text{exact}} - v_i^{\text{approx}}|^2}{N}} \end{array} \right\} \quad (17)$$

where:

$$\delta \xi = \frac{|b-a|}{N}$$

For instance take the governing equation given in equation (1) as well as the initial and boundary conditioned provided in equations (2)-(3) with varying parameters as follows:

**Test problem.** We consider HD model equation given in equation (18) and its exact analytical solution given

**Table 2.** Comparative analysis of  $L_\infty(v)$  error at time  $t = 0.005$  for some  $\zeta$  values associated with given test problem

RBF	T values	$\zeta$ values	$\zeta$ values	$L_\infty(v)$	$L_\infty(v)$ [10]
MQ	0.001	0.11	135	$7.382 \times 10^{-4}$	$4.118 \times 10^{-4}$
	0.002			$1.477 \times 10^{-3}$	$1.900 \times 10^{-3}$
	0.003			$2.215 \times 10^{-3}$	$4.000 \times 10^{-3}$
	0.004			$2.954 \times 10^{-3}$	$2.700 \times 10^{-3}$
	0.005			$3.692 \times 10^{-3}$	$5.700 \times 10^{-3}$
IMQ	0.001	4.50	1760	$8.580 \times 10^{-4}$	$4.319 \times 10^{-4}$
	0.002			$1.716 \times 10^{-3}$	$2.600 \times 10^{-3}$
	0.003			$2.574 \times 10^{-3}$	$3.100 \times 10^{-3}$
	0.004			$3.433 \times 10^{-3}$	$6.200 \times 10^{-3}$
	0.005			$4.291 \times 10^{-3}$	$6.700 \times 10^{-3}$
GA	0.001	0.12	1760	$8.874 \times 10^{-4}$	$2.618 \times 10^{-4}$
	0.002			$1.775 \times 10^{-3}$	$9.823 \times 10^{-4}$
	0.003			$2.663 \times 10^{-3}$	$1.700 \times 10^{-3}$
	0.004			$3.550 \times 10^{-3}$	$2.400 \times 10^{-3}$
	0.005			$4.438 \times 10^{-3}$	$3.100 \times 10^{-3}$
IQ	0.001	0.08	115	$7.338 \times 10^{-4}$	$2.034 \times 10^{-4}$
	0.002			$1.468 \times 10^{-3}$	$1.700 \times 10^{-3}$
	0.003			$2.202 \times 10^{-3}$	$1.800 \times 10^{-3}$
	0.004			$2.936 \times 10^{-3}$	$4.500 \times 10^{-3}$
	0.005			$3.670 \times 10^{-3}$	$5.300 \times 10^{-3}$

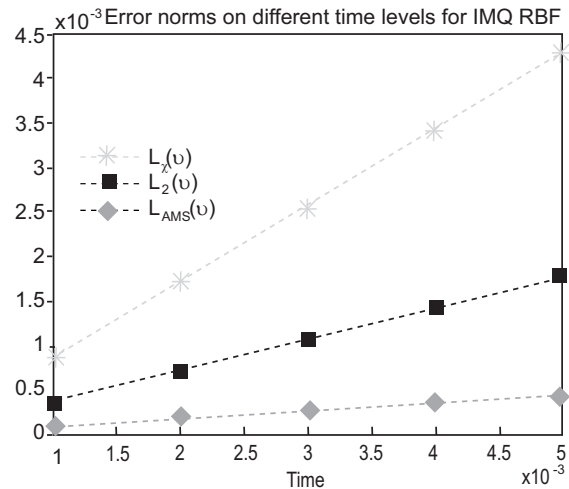
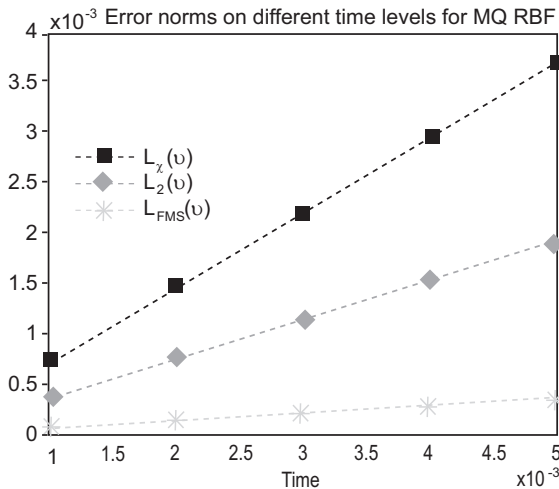


**Fig. 1.** Graphical overview of  $L_\infty(v)$ ,  $L_2(v)$  and  $L_{RMS}(v)$  error norm for MQ and IMQ RBF (left and right) at time for a some  $t = 0.005$  for a some  $\zeta$  values associated with Table 7 for given test problem.

in equation (19), with parameters  $\eta=4, \gamma=1$  over space and time interval  $[0,1] \times [0,0.005]$  respectively and the values of the step size  $\delta x=h=0.1$  and time step  $\delta t=0.001$ . We have employed multiquadric (MQ)  $\Phi(r) = \sqrt{1 + (\zeta r)^2}$ , Inverse multiquadric (IMQ)  $\Phi(r) = \frac{1}{\sqrt{1 + (\zeta r)^2}}$ , Gaussian (GA)  $\Phi(r) = e - (\zeta r)^2$  and Inverse

quadratic (IQ)  $\Phi(r) = \frac{1}{1 + (\zeta r)^2}$  radial basis functions with the shape parameter  $\zeta$ , whose ideal value was determined by the algorithm previously stated. Tables 2 and Fig. 1-2 shows the findings of our suggested approach compared to earlier methods described in literature, respectively.

**Table 3.** Comparative analysis of  $L_2(v)$  error at time  $t = 0.005$  for some  $\zeta$  values associated with given test problem

RBF	T values	$\zeta$ values	$\zeta$ values	$L_\infty(v)$	$L_\infty(v)$ [10]
MQ	0.001	0.11	135	$3.840 \times 10^{-4}$	$1.892 \times 10^{-4}$
	0.002			$7.684 \times 10^{-4}$	$8.738 \times 10^{-4}$
	0.003			$1.153 \times 10^{-3}$	$2.500 \times 10^{-3}$
	0.004			$1.538 \times 10^{-3}$	$1.600 \times 10^{-3}$
	0.005			$1.924 \times 10^{-3}$	$2.500 \times 10^{-3}$
IMQ	0.001	4.50	1760	$3.531 \times 10^{-4}$	$2.457 \times 10^{-4}$
	0.002			$7.065 \times 10^{-4}$	$1.600 \times 10^{-3}$
	0.003			$1.060 \times 10^{-3}$	$1.800 \times 10^{-3}$
	0.004			$1.414 \times 10^{-3}$	$3.500 \times 10^{-3}$
	0.005			$1.769 \times 10^{-3}$	$4.000 \times 10^{-3}$
GA	0.001	0.12	1760	$3.624 \times 10^{-4}$	$1.495 \times 10^{-4}$
	0.002			$7.250 \times 10^{-4}$	$6.893 \times 10^{-4}$
	0.003			$1.088 \times 10^{-3}$	$1.300 \times 10^{-3}$
	0.004			$1.451 \times 10^{-3}$	$2.000 \times 10^{-3}$
	0.005			$1.814 \times 10^{-3}$	$2.600 \times 10^{-3}$
IQ	0.001	0.08	115	$3.550 \times 10^{-4}$	$1.295 \times 10^{-4}$
	0.002			$7.103 \times 10^{-4}$	$1.200 \times 10^{-3}$
	0.003			$1.066 \times 10^{-3}$	$1.200 \times 10^{-3}$
	0.004			$1.422 \times 10^{-3}$	$3.000 \times 10^{-3}$
	0.005			$1.778 \times 10^{-3}$	$3.700 \times 10^{-3}$

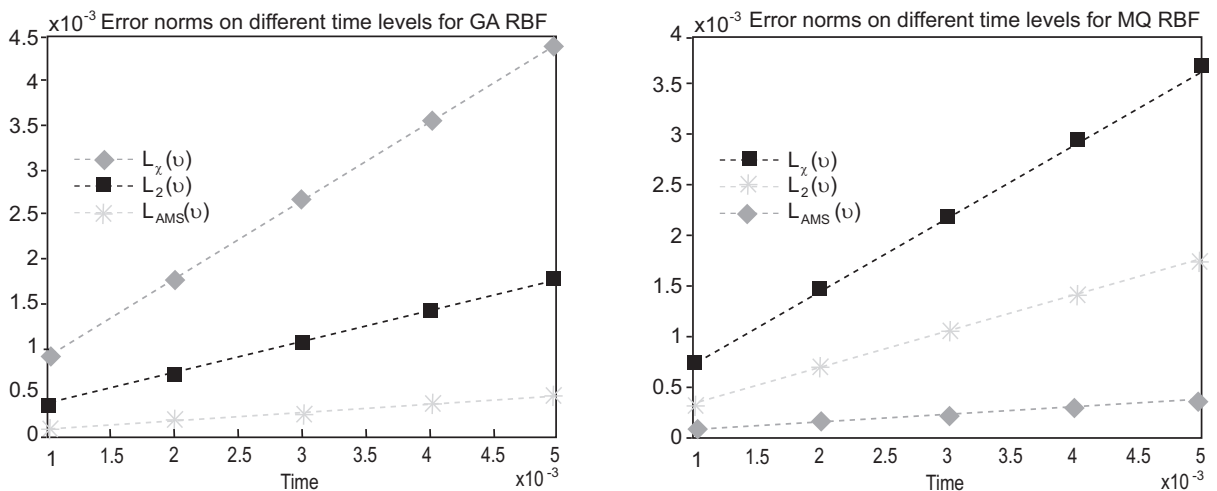


**Fig. 2.** Graphical overview of  $L_\infty(v)$ ,  $L_2(v)$  and  $L_{RMS}(v)$  error norm for GA and IQ RBF (left and right) at time  $t = 0.005$  for a some  $\zeta$  values associated with table 8 for given test problem.

**Table 4.** Comparative analysis of  $L_{RMS}$  (v) error at time  $t=0.005$  for some  $\zeta$  values associated with given test problem

RBF	T values	$\zeta$ values	$\zeta$ values	$L_{RMS}$ (v)	$L_{RMS}$ (v) [10]
MQ	0.001	0.11	135	$7.382 \times 10^{-5}$	$1.8037 \times 10^{-4}$
	0.002			$1.477 \times 10^{-4}$	$8.328 \times 10^{-4}$
	0.003			$2.215 \times 10^{-4}$	$2.400 \times 10^{-3}$
	0.004			$2.954 \times 10^{-4}$	$1.500 \times 10^{-3}$
	0.005			$3.692 \times 10^{-4}$	$2.400 \times 10^{-3}$
IMQ	0.001	4.50	1760	$8.580 \times 10^{-5}$	$2.343 \times 10^{-4}$
	0.002			$1.716 \times 10^{-4}$	$1.500 \times 10^{-3}$
	0.003			$2.574 \times 10^{-4}$	$1.700 \times 10^{-3}$
	0.004			$3.433 \times 10^{-4}$	$3.300 \times 10^{-3}$
	0.005			$4.291 \times 10^{-4}$	$3.800 \times 10^{-3}$
GA	0.001	0.12	1760	$8.874 \times 10^{-5}$	$1.426 \times 10^{-4}$
	0.002			$1.775 \times 10^{-4}$	$6.572 \times 10^{-4}$
	0.003			$2.663 \times 10^{-4}$	$1.300 \times 10^{-3}$
	0.004			$3.550 \times 10^{-4}$	$1.900 \times 10^{-3}$
	0.005			$4.438 \times 10^{-4}$	$2.500 \times 10^{-3}$
IQ	0.001	0.08	115	$7.338 \times 10^{-5}$	$1.235 \times 10^{-4}$
	0.002			$1.468 \times 10^{-4}$	$1.100 \times 10^{-3}$
	0.003			$2.202 \times 10^{-4}$	$1.200 \times 10^{-3}$
	0.004			$2.936 \times 10^{-4}$	$2.900 \times 10^{-3}$
	0.005			$3.670 \times 10^{-4}$	$3.500 \times 10^{-3}$

## Conclusion

In this paper, RBF for solitary wave model equations, such as Harry Dym (HD) equation is examined and discussed in detail along with some basic concepts and definitions. A numerical scheme known as the localized RBF meshless approach is utilized to resolve the aforementioned model. The Runge-Kutta (RK-4) time stepping strategy is utilized to carry out the temporal variable in the specified model equation. To evaluate the accuracy of our suggested technique, we have calculated  $L_{RMS}$ ,  $L_{\infty}$  and  $L_2$  error norms, tables and graphs. Our methodology structure to other existing numerical methods, is less difficult and more straightforward to treat any higher order nonlinear PDEs. This method has several major advantages over others, including convergence rate, stability, sparse and local differentiation matrices, and reasonable processing cost. Remarkably, it is clear from our findings that we attain higher accuracy using very small values of the shape parameter  $\zeta$  with the help of mentioned algorithm, than the so large values previously employed in literature. Moreover, it can be used with other types of integral and non-integral PDEs.

## Acknowledgment

The authors are thankful to the reviewers for their constructive and valuable comments.

**Conflict of Interest.** The authors declare that they have no conflict of interest.

## References

- Assabaai, M.A. 2021. Numerical solution of the Harry Dym equation using Chebyshev spectral method via Lie group method, IOP Publishing. *Journal of Physics: Conference Series*, **1900**: 012004. DOI: <https://doi.org/10.1088/1742-6596/1900/1/012004>
- Assabaai, M.A., Mukherij, O.F. 2020. Exact solutions of the Harry Dym equation using Lie group method, University of Aden. *Journal of Natural and Applied Sciences*, **24**: 481-487. DOI: <https://doi.org/10.47372/uajnas.2020.n2.a15>
- Broer, L.J.F. 1975. Approximate equations for long water waves. *Applied Scientific Research*, **31**: 377-395. DOI: <https://doi.org/10.1007/BF00418048>
- Fonseca, F. 2017. A solution of the harry-dym equation using lattice-boltzmann and a solitary wave methods. *Applied Mathematical Sciences*, **11**: 2579-2586. DOI: <https://doi.org/10.12988/ams.2017.79280>
- Franke, C., Schaback, R. 1998a. Convergence order estimates of meshless collocation methods using radial basis functions. *Advances in Computational Mathematics*, **8**: 381-399. DOI: <https://doi.org/10.1023/A:1018916902176>

- Franke, C., Schaback, R. 1998b. Solving partial differential equations by collocation using radial basis functions. *Applied Mathematics and Computation*, **93**: 73-82. DOI: [https://doi.org/10.1016/S0096-3003\(97\)10104-7](https://doi.org/10.1016/S0096-3003(97)10104-7)
- Franke, R. 1982. Scattered data interpolation: tests of some methods. *Mathematics of Computation*, **38**: 181-200. DOI: <https://doi.org/10.1090/S0025-5718-1982-0637296-4>
- Fuchssteiner, B., Schulze, T., Carillo, S. 1992. Explicit solutions for the Harry-Dym equation. *Journal of Physics A: Mathematical and General*, **25**: 223. DOI: <https://doi.org/10.1088/0305-4470/25/1/025>
- Gesztesy, F., Unterkofler, K. 1992. Iso-spectral deformations for Sturm-liouville and Dirac-type operators and associated nonlinear evolution equations. *Reports on Mathematical Physics*, **31**: 113-137. DOI: [https://doi.org/10.1016/0034-4877\(92\)90008-O](https://doi.org/10.1016/0034-4877(92)90008-O)
- Ghiassi, E.K., Saleh, R. 2017. A mathematical approach based on the homotopy analysis method: application to solve the nonlinear Harry-dym (HD) equation. *Applied Mathematics*, **8**: 1546-1562. DOI: <https://doi.org/10.4236/am.2017.811113>
- Hardy, R.L. 1971. Multiquadric equations of topography and other irregular surfaces. *Journal of Geophysical Research*, **76**: 1905-1915. DOI: <https://doi.org/10.1029/JB076i008p01905>
- Kadomtsev, B.B., Petviashvili, V.I. 1970. On the stability of solitary waves in weakly dispersing media. *Doklady Akademii Nauk SSSR*, **192**: 753-756.
- Kansa, E.J. 1990a. Multiquadrics-a scattered data approximation scheme with applications to computational fluid-dynamics-I surface approximations and partial derivative estimates. *Computers and Mathematics with Applications*, **19**: 127-145. DOI: [https://doi.org/10.1016/0898-1221\(90\)90270-T](https://doi.org/10.1016/0898-1221(90)90270-T)
- Kansa, E.J. 1990b. Multiquadrics-a scattered data approximation scheme with applications to computational fluid-dynamics-II solutions to parabolic, hyperbolic and elliptic partial differential equations. *Computers and Mathematics with Applications*, **19**: 147-161. DOI: [https://doi.org/10.1016/0898-1221\(90\)90271-K](https://doi.org/10.1016/0898-1221(90)90271-K)
- Kaup, D. 1975. A higher-order water-wave equation and the method for solving it. *Progress of Theoretical Physics*, **54**: 396-408. DOI: <https://doi.org/10.1143/PTP.54.396>
- Korteweg, D.J., de Vries, G. 2009. *XLI. On the Change of Form of Long Waves Advancing in a Rectangular Canal and on a New Type of Long Stationary Waves*, pp. 422-443, Published on line, 8 May, 2009, UK. DOI: <https://doi.org/10.1080/14786449508620739>
- Kruskal, M.D., Moser, J. 1975. Dynamical systems, theory and applications. *Lecture Notes in Physics*, **38**: 310-354. DOI: <https://doi.org/10.1007/3-540-07171-7>
- Kupershmidt, B. 1985. Mathematics of dispersive water waves. *Communications in Mathematical Physics*, **99**: 51-73. DOI: <https://doi.org/10.1007/BF01466593>
- Li, H., Xu, J. 2020. On the double-pole and two-soliton solutions of the Harry-dym equation. *Applied Mathematics Letters*, **104**: 106276. DOI: <https://doi.org/10.1016/j.aml.2020.106276>
- Madych, W.R., Nelson, S.A. 1992. Bounds on multivariate polynomials and exponential error estimates for multiquadric interpolation. *Journal of Approximation Theory*, **70**: 94-114. DOI: [https://doi.org/10.1016/0021-9045\(92\)90058-V](https://doi.org/10.1016/0021-9045(92)90058-V)
- Madych, W.R., Nelson, S.A. 1990. Multivariate interpolation and conditionally positive definite functions-II. *Mathematics of Computation*, **54**: 211-230. DOI: <https://doi.org/10.1090/S0025-5718-1990-0993931-7>
- Micchelli, C.A. 1984. *Interpolation of Scattered Data: Distance Matrices and Conditionally Positive Definite Functions*, pp. 143-145, Springer, The Netherlands. DOI: [https://doi.org/10.1007/978-94-009-6466-2\\_7](https://doi.org/10.1007/978-94-009-6466-2_7)
- Mokhtari, R. 2011. Exact solutions of the Harry-dym equation. *Communications in Theoretical Physics*, **55**: 204. DOI: <https://doi.org/10.1088/0253-6102/55/2/03>
- Nadjafikhah, M., Kabi-Nejad, P. 2013. Approximate symmetries of the Harry-dym equation. *Mathematical Physics*, **2013**: 109170. DOI: <http://dx.doi.org/10.1155/2013/109170>
- Novikov, D.P. 1999. Algebraic-geometric solutions of the Harry-dym equation. *Siberian Mathematical Journal*, **40**: 136-140. DOI: <https://doi.org/10.1007/BF02674299>
- Rawashdeh, M. 2014. A new approach to solve the fractional Harry-dym equation using the FRDTM. *International Journal of Pure and Applied Mathematics*, **95**: 553-566. DOI: <http://dx.doi.org/10.12732/ijpam.v95i4.8>
- Rippa, S. 1999. An algorithm for selecting a good value for the parameter C in radial basis function

- interpolation. *Advances in Computational Mathematics*, **11**: 193-210. DOI: <https://doi.org/10.1023/A:1018975909870>
- Scheuerer, M. 2011. An alternative procedure for selecting a good value for the parameter  $c$  in RBF-interpolation. *Advances in Computational Mathematics*, **34**: 105-126. DOI: <https://doi.org/10.1007/s10444-010-9146-3>
- Tarwater, A.E. 1985. Parameter Study of Hardy's Multiquadric Method for Scattered Data Interpolation (No.UCRL-53670). Lawrence Livermore National Lab., CA, USA.
- Taufiq, M., Uddin, M. 2021. Numerical solution of fractional order anomalous subdiffusion problems using radial kernels and transform. *Journal of Mathematics*, 1-9. DOI: <https://doi.org/10.1155/2021/9965734>
- Trahan, C.J., Wyatt, R.E. 2003. Radial basis function interpolation in the quantum trajectory method: optimization of the multi-quadric shape parameter. *Journal of Computational Physics*, **185**: 27-49. DOI: [https://doi.org/10.1016/S0021-9991\(02\)00046-3](https://doi.org/10.1016/S0021-9991(02)00046-3)
- Trefethen, L.N. 2000. *Spectral Methods in MATLAB*, pp. 160, SIAM Publisher, Philadelphia.
- Uddin, M., Taufiq, M. 2019a. Approximation of time fractional Black-scholes equation via radial kernels and transformations. *Fractional Differential Calculus*, **9**: 75-90. DOI: <https://doi.org/10.7153/fdc-2019-09-06>
- Uddin, M., Taufiq, M. 2020. On the local transformed based method for partial integro-differential equations of fractional order. *Miskolc Mathematical Notes*, **21**: 435-449. DOI: <https://doi.org/10.18514/MMN.2020.3125>
- Uddin, M., Taufiq, M. 2019b. On the approximation of volterra integral equations with highly oscillatory Bessel kernels via Laplace transform and quadrature. *Alexandria Engineering Journal*, **58**: 413-417. DOI: <https://doi.org/10.1016/j.aej.2018.12.003>
- Vasconcelos, G.L., Kadanoff, L.P. 1991. Stationary solutions for the Saffman-taylor problem with surface tension. *Physical Review A*, **44**: 6490. DOI: <https://doi.org/10.1103/PhysRevA.44.6490>
- Whitham, G.B. 1967. Variational methods and applications to water waves. In: *Proceedings of the Royal Society of London-Series A: Mathematical and Physical Sciences*, **299**: 6-25. DOI: <https://doi.org/10.1098/rspa.1967.0119>
- Xiao, Y., Fan, E., 2019. Long time behaviour and soliton solution for the Harry-dym equation. *Journal of Mathematical Analysis and Applications*, **480**: 123248. DOI: <https://doi.org/10.1016/j.jmaa.2019.06.019>